Journal of Urban and Environmental Engineering, v.19, n.1, p.57-68

ISSN 1982-3932
doi: 10.4090/jueev19n1.2025.057068

Journal of Urban and Environmental Engineering

www.journal-uee.org

ANALYSIS OF URBAN HEAT ISLAND EFFECT IN THIRUVANANTHAPURAM DISTRICT – A SOUTHERNMOST PENINSULAR REGION OF INDIA

Ashida Shabeer*, K. Swarnalatha and Shilpa S. Nair

Department of Civil Engineering, College of Engineering Trivandrum, India

Received 7 October 2024; received in revised form 16 May 2025; accepted 18 May 2025

Abstract: Urban areas are significant contributors of local and regional climatic changes. The Urban Heat Island (UHI) formation can influence the microclimate of urban areas, making them warmer than the surrounding regions. The temporal and spatial variation of UHI effect in a typical southernmost peninsular part of India was studied for around two decades using geospatial techniques. The Land Surface Temperature (LST) was found using ETM+ and OLI/TIRS satellite imagery. The Ecological Evaluation Index (EEI) is a tool that can be used to assess an area's ecological quality based on human comfort, from excellent to worst zones. Urban Thermal Field Variance Index (UTFVI) is a term that can be used to scale the intensity of UHI based on EEI. It was observed from the study that the UHS was mostly concentrated in the central business region of the study area. It was also seen that over the years, although there was a reduction in the area of urban hotspots, an increase in the area of worst zones according to UTFVI classification happened. Shifting of zones from 'excellent' to 'worst' areas was also observed. UHI and Urban Cool Islands (UCI) are identified. The study will be highly helpful in realizing the climatic changes happening in this region and adopting preventive measures in a systematic way based on the baseline data generated.

Keywords: Urban heat island; land surface temperature; Ecological Evaluation Index; Urban Thermal Field Variance Index; urban hotspots.

* Correspondence to: K. Swarnalatha, Tel.: +91 9495629708. E-mail: swarnalatha@cet.ac.in

INTRODUCTION

Rapid changes in the land use pattern have led to global deterioration of environmental quality. The Urban areas have become major contributors to regional and local climatic change (Li *et al*., 2022). Urbanization has significantly changed the structure of human habitation, which has enhanced urban economic activity and produced several adverse environmental effects, including CO_2 emissions. According to UN Department of Economic and Social Affairs (UN DESA) 2018, about half of world's population belongs to urbanized areas and by the year 2050, it is predicted that it will increase to 68%. The global urban area increased by 168% between 2001 and 2018, with Asia and Africa experiencing the largest growth rates (World Cities Report 2020). In India, 32% people i.e., approximately 7% of total world population live in urban areas (Raj *et al*., 2020). The reduction of green spaces is a result of rapid urbanization which has replaced natural vegetation with impermeable surfaces that trap heat and release it into the atmosphere (Abulibdeh *et al*., 2021).The expansion of urban areas is considered as a significant factor for the increase in Land Surface Temperature (LST) (Ayanlade *et al*., 2021).LST is the radiative skin temperature of the land caused by, and building density (Mustafa *et al*., 2020). Forests and agricultural land reduce LST while settlement and fallow land with dry surface accelerate the LST (Pandey *et al*., 2022). The influence of LST on the energy exchange between the earth's surface and atmosphere is crucial for understanding environmental changes. LST is an important parameter used for the retrieval of climatic variables solar radiation (Khan *et al*., 2021). The intensity of LST is directly related to the rate of urbanization, land use patterns, such as air temperature and water vapour (Glynn *et al*., 2019).

LST is extracted from thermal infrared (TIR) spectral data taken by sensors mounted on the ground, in the air, or on satellites. The thermal signal of the satellite remote sensing measures the LST at regional and global scale with high spatial and temporal resolutions (Yuling *et al*., 2023). LST is a common tool to identify ecological comfort zones and urban heat islands. The LST can be estimated from the satellite images. Mainly used images are the Landsat images, Moderate Resolution Imaging Spectroradiometer (MODIS) and Sentinel. Determination of LST is the first and significant stage in the study of the UHI.

UHI effect is the phenomenon in which temperature tends to be higher in urban regions than the surrounding non-urban areas (Sidiqui *et al*., 2022, Faisal *et al*., 2021, Almeida *et al*., 2021). The development of urban areas leads to the formation of UHI. (Elmarakby *et al*., 2020). It is a major microclimate phenomenon caused by the introduction of built-up areas, impervious construction materials, along with anthropogenic sources of heating, such as automobiles and power plants (Vahmani *et al*., 2022). UHI phenomena were first observed in London by Luke Howard (Amit *et al*., 2021). The UHI impact is influenced by the decline of vegetation and the transformation of pervious regions into built up and impermeable regions (Rendana *et a*l., 2023). UHI zones are more concentrated, near the urban economic centres with dense populations (Rashid *et al*., 2022). Most of the city areas have an increasing trend of LST and are on the verge of becoming UHI regions. Population, lack of greenery, and anthropogenic forcing were the main factors affecting UHI (Dewan *et al*., 2021). The change of Land Cover increases built-up regions by reducing vegetation and water bodies, which further enhances the LST resulting in UHI phenomena. Remote sensing and geospatial techniques are highly efficient to study the relationship between LST and UHI. The high resolution and extensive coverage of remote sensing technique help in identifying the UHIs (David *et al*., 2023).

Land Cover indices such as Normalized difference vegetation index (NDVI), Normalized difference built-up index (NDBI), Normalized difference bareness index (NDBal), Normalized difference moisture index (NDMI), and Modified normalized difference water index (MNDWI) are used in the LST related studies to evaluate their effect on the ecological condition of the urban areas (Shahfahad *et al*., 2021). A positive linear correlation was observed between Built-up area and barren land with LST, while negative correlation was observed between vegetation, water bodies, impervious area (Tesfamariam *et al*., 2023). NDVI show a stronger negative correlation and NDWI show a stronger positive correlation with LST. NDBI present a stronger positive correlation. NDBAI have positive relationship with LST (Guha *et al*., 2020). The correlation analysis showed that NDBI and albedo showed a positive correlation with LST (Kikon *et al*., 2017).

Urban environmental quality is a measurable indicator of the extent to which an environment can meet the needs of urban dwellers (Mohammad *et al*., 2020). It has an impact on the comfort and quality of human life while taking into account the UHI effect (Kusumawardani *et al*., 2023). Urban thermal comfort is evaluated using Urban Thermal Field Variance Index (UTFVI). (Sharma *et al*., 2021). It is one of the most prevalent and reliable indices used to assess the environmental quality or thermal comfort of the urban centres. Itquantifies the thermal ecological conditions of urban areas in terms of LST (Moisa *et al*., 2022). The areas which were covered with different vegetation types had an optimal microclimate. The area covered with impervious surface of urban areas dominated by built-up areas respectively showed thermal discomfort (Tesfamariam *et al*., 2023). The urban thermal

environments are getting worse because of the rising urbanisation. Urban hotspots (UHS) are the areas with the intense thermal conditions recorded on higher LST surfaces. It occurs in small pockets of densely populated areas or bare soil areas that are excessively hot and unsuitable for human habitation (Shahfahad *et al*., 2021). Hotspots are most common in heavily populated and built-up regions and can have a serious impact on UHI. The UHS are the locations with significant economic growth and are crucial to the competitiveness of the entire city (Li *et al*., 2018).

The present study focuses on the study of variation of spatio-temporal analysis of UTFVI of a typical southernmost peninsular region of India. The extent of urban heat island effect in the study area is found out and the urban hotspots as of the latest period are identified. A correlational analysis is conducted with LST and the land use indices and a mathematical model of LST is developed.

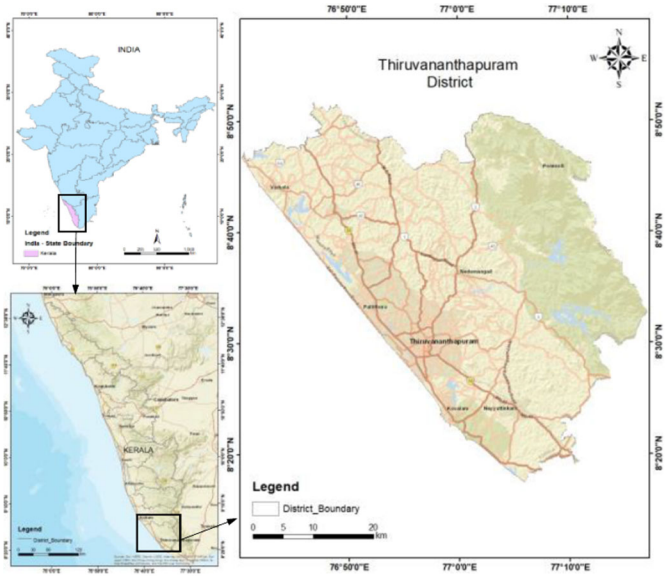

Fig. 1. Representation of study área

Study Area

The study area (**Fig. 1**) is Thiruvananthapuram district of Kerala, India which is the southernmost peninsular region of India situated between the latitude and longitude of 8.5241° N and 76.9366° E respectively. It spreads through an area of 2192km2. Thiruvananthapuram has a tropical climate. The district has 11 blocks, 4 municipalities and 1 corporation. It is the second most populous district following Malappuram district. It is subdivided into 6 sub districts or taluks namely Thiruvananthapuram, Chirayinkeezhu, Neyyatinkara, Nedumangadu, Varkala and Kattakada. The urban bodies include Thiruvananthapuram Corporation and Varkala, Neyyatinkara, Attingal, Kattakada and Nedumangadu are the municipalities.

Methodology

The satellite images were downloaded from USGS Earth Explorer. Landsat 8-OLI/TIRS and Landsat 7 satellite images were used. Collection 1 Level-1 data were used. A period of approximately 2 decades is chosen from 2001 to 2023. Maps are prepared for the years 2001, 2015 and 2023. Landsat 8 was used for the period of 2015 and 2023. Landsat 7 was used for the period 2001. Image analysis was performed on ArcGIS (ArcMap 10.8).

Retrieval of LST

LST is calculated using the thermal bands viz., Band 10 being the thermal band for Landsat 8-9 and Band 6, the thermal band for Landsat 4-7.LST values are calculated using Landsat 8 Operational Land Imager (OLI)/Thermal Infrared Sensor (TIRS) Collection 1 Level-1 data. There are two TIRS bands where band 10 is the TIRS-1 having a wavelength from 10.6 to 11.19 µm. The TIRS-2 is the band 11 having a wavelength from 11.50 to 12.51 µm (usgs.gov). The conversion of Digital Number (DN) to Spectral Radiance (SR) is done using the equations mentioned in Landsat 8 (L8) and Landsat 7 (L7) Data Users Handbook Version 2, 2019 as given in equation 1 and 2.

For Landsat 8-9

$$L\lambda = M_L * \mathrm{Q_{cal}} + A_L \quad (1)$$

For Landsat 4-7

$$L_\lambda = \left(\frac{L_{\max\lambda} - L_{\min\lambda}}{Q_{\mathrm{cal\,max}} - Q_{\mathrm{cal\,min}}}\right)(Q_{\mathrm{cal}} - Q_{\mathrm{cal\,min}}) + L_{\min\lambda} \quad (2)$$

where L_λ is the Spectral radiance, Lmax and Lmin are the maximum and minimum SR respectively, ML is the Radiance Multiplicative band which is equal to 0.000342, A_L is the Radiance Additive Band which is equal to 0.1000, Q_{cal} is quantized calibrated pixel value in DN, Qcalmax is the maximum quantized calibrated pixel value in DN and Qcalmin is the minimum quantized calibrated pixel value in DN.

The Radiance multiplicative and addition band is obtained from the metafile data of the satellite image. The SR is converted to brightness temperature (BT) in °C as in equation (3) defined in the Landsat Data Users Handbook.

$$\mathrm{BT} = \mathrm{K2}/\left(\ln\left(\frac{\mathrm{K1}}{\mathrm{L}\lambda + 1}\right) - 273.15\right) \quad (3)$$

where K1 and K2 are thermal conversion constants and obtained from metadata files.

Proportion of vegetation (P_v) (Guha *et al*., 2020) is defined as the percentage of an area under vegetation or another form of soil (Equation 4).

$$P_v = S_q \left(\frac{NDVI - NDVI_{min}}{NDVI_{max} - NDVI_{min}} \right) \quad (4)$$

The Land Surface Emissivity (ε) is calculated by the equation as described by Naim *et al*. (2021).

$$\varepsilon = 0.004 \times P_v + 0.986 \quad (5)$$

LST is calculated as described by Moisa *et al*. (2022).

$$LST = \left(\frac{BT}{1} \right) + W \times \left(\frac{BT}{14,380} \right) \times \ln(\varepsilon) \quad (6)$$

For Landsat 8, W=10.8 μm and for Landsat 5 and 7, W =11.457 μm

The comparison of the calculated LST was made with the air temperature obtained from the Central Pollution Control Board data from the two available stations.

Calculation of UTFVI

The range of UTFVI can be categorized into six classes, ranging from 'excellent' to 'worst', according to the Ecological Evaluation Index (EEI). The index, which analyses the UHI effect on the quality of urban life as explained by Sharma *et al*., 2020.

$$UTFVI = \frac{T_s - T_{mean}}{T_{mean}} \quad (7)$$

where Ts is LST and T*mean* is the mean of LST.

The Threshold UTFVI value for ecological evaluation and thermal comfort is discussed by Shahfahad *et al*., 2021 and Omali 2020. UHS are the localized hotspots within urban heat islands that are uncomfortable for human activities. UHS typically occurs in discrete densely built-up areas or in bare-soil regions. These small pockets are mapped using the equation studied by *Abir et a*l. (2021).

$$LST \geq \mu + 2\sigma \quad (8)$$

The UHI and non-UHI regions are classified by the equations studied by Guha *et al*., 2018.

$$\begin{aligned} &ST > \mu + 0.5 * \sigma \\ &0 < LST \leq \mu + 0.5 * \sigma \end{aligned} \quad (9)$$

where, μ and σ are the mean and SD of LST respectively A standard deviation segmenting method is used to determine the UHI effect from the LST map. UHI and Urban Cool Islands (UCI) were found out. Various UHI classes are discussed by Xiong *et al*., 2022.

LULC Change Analysis

The LULC (Land Use/Land Cover) analysis for the Thiruvananthapuram city for the years 2001 and 2023 were done using Landsat satellite image of green, red and near-infrared bands by maximum likelihood classification.

Urbanization Proportion Index (UPI)

UPI (Urbanisation Proportion Index) indicates the magnitude of urban growth over a time period. It can be expressed using the equation (Suja *et al*., 2013):

$$UTPI = \left(\frac{ULAt + n - ULAt}{TLA} \right) 100 \quad (10)$$

Where ULAt+n is the area of urban land for year t+n, ULAt is the area of urban land for year t, n is the number of years and TLA is the total land area.

The UPI was calculated for Thiruvananthapuram city area for a period of 22 years from 2001-2023.

Determination of Land Use Indices and Albedo

Optical bands were used for this purpose. Equations for Land use indices are obtained from the United States Geological Survey website.

NDVI

NDVI measures the in vegetation as given Equation 11. NDVI values lie between -1 and 1. Positive value denotes dense vegetation whereas negative values indicate clear and sparse soils.

$$NDVI = \frac{NIR - R}{NIR + R} \quad (11)$$

where NIR is the Near Infrared band and R is the red band. For Landsat 8 and 9, Band 5 and 4 is taken as NIR and R respectively whereas for Landsat 4-7, Band 4 and 3.

NDBI

NDBI is used to find the built-up regions from satellite imagery. It is calculated by using the optical bands of the Short Wave Infra-Red (SWIR) and the NIR band. The NDBI value ranges between − 1 and+1. A positive value denotes built-up regions whereas a negative value denotes vegetation and water bodies.

$$NDBI = \frac{SWIR - NIR}{SWIR + NIR} \quad (12)$$

For Landsat 8 and 9, Band 6 is the SWIR and Band 5 is the NIR whereas for Landsat 4-7, Band 5 is the SWIR and Band 4 is the NIR.

NDBaI

NDBaI is used for the identification of the bare regions. It is estimated to be from the optical bands of the SWIR

and the Thermal infrared (TIR) band. The values range between +1 and -1.

$$NDBal = \frac{SWIR - TIR}{SWIR + TIR} \quad (13)$$

For Landsat 8 and 9, Band 6 is the SWIR and Band 10 is the TIR For Landsat 4-7, Band 5 is the SWIR and Band 6 is the TIR

3.5.4 MNDWI

MNDWI is used to identify the open water features. It is determined from the optical bands of the Green and SWIR band. The values lie between −1 and +1, with positive value indicating water bodies or humidity and negative values indicating dry regions.

$$MNDVWI = \frac{GREEN - SWIR}{GREEN + SWIR} \quad (14)$$

For Landsat 8 and 9, Band 3 is the Green and Band 6 is the SWIR. For Landsat 4-7, Band 2 is the Green and Band 5 is the SWIR

NDMI

NDMI is used to determine moisture content present in vegetation. It is calculated by using the NIR and SWIR band. Lower value indicates lack of moisture in plants whereas higher values indicate higher vegetation moisture. It indicates the wetness or dryness of an area. Value ranges from -1 to +1.

$$NDMI = \frac{NIR - SWIR}{NIR + SWIR} \quad (15)$$

For Landsat 8 and 9, Band 5 is the NIR and Band 6 is the SWIR. For Landsat 4-7, Band 4 is the NIR and Band 5 is the SWIR. The albedo (α) is calculated from the equation as studied by Kikon *et al*. (2017).

Statistical analysis of data

Correlational studies and Multivariate linear regression model were developed with Land use Indices, Albedo and LST. A Pearson's correlation analysis was performed between Land Use Indices such as NDVI, NDBI, NDBaI, MNDWI and NDMI along with albedo with LST. Multivariate linear regression models are an important tool to analyze the relationship between dependent and independent variables.

$$y = a0 + a1X1 + a2X2 + a3X3 + a4X4 \quad (16)$$

Here, y is the dependent variable (LST), a0 is the constant, and X1, X2, X3, and X4 are the determining variables such as the land use parameters and a1, a2, a3, and a4 are the coefficients that describe the influence on variables. A model is developed with LST as dependent variable whereas Land use Indices and albedo are the explanatory variables. The positive and negative coefficients of the explanatory variable indicate an increase or decrease in LST with the particular variable. For the validation of modelled data, Root Mean Square Error (RMSE) is found out (Equation 17).

$$RMSE = \sqrt{\sum_{I=1}^{n} (y - y_i)^2 / n} \quad (17)$$

Where y and, *yi* are the predicted and observed value respectively and n being the number of observations.

RESULTS AND DISCUSSIONS

The spatio-temporal analysis of the various parameters including UTFVI, UHS, UHI and UCI over a span of two decades was done from the LST maps. The variation of Land Use Indices such as NDVI, NDBI, NDBaI, MNDWI, NDMI and albedo were studied. A correlational analysis of the Land Use indices and Albedo were done with LST.

Multivariate Linear Regression Model (MLR) was obtained for LST.

Determination of LST

The LST of the study area was calculated by the methodology discussed in 3.1. The variability of LST for the study period is shown in **Fig. 2**. LST value observed for the year 2001 had a minimum value of 17.621°C and a maximum of 29. 455°C. During 2015, the minimum value observed was 19.146°C and a maximum value of 33.415°C was obtained. For the year 2023, the minimum and maximum value obtained was 19.905°C and 37.093°C respectively.

There is an overall increase in average temperature of about 5°C for a span of 22 years. Similar range of LST was obtained for a municipality of Kollam district located nearer to the study area (Satheendran *et al*., 2018) also. The classified LST of 2001, 2015 and 2023 is shown in **Fig. 3**. The range of LST is subdivided as < 21°C, 21 - 23°C, 23-25°C, 25-27°C and > 27°C. It is observed that there is a substantial increase in the areas having LST values greater than 27°C.

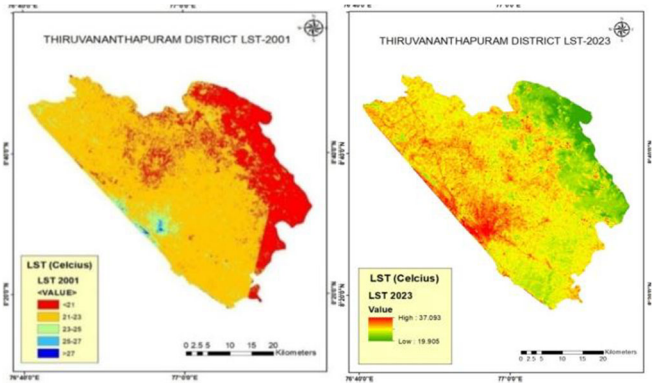

Fig. 2 LST for (a) 2001 and (b) 2023

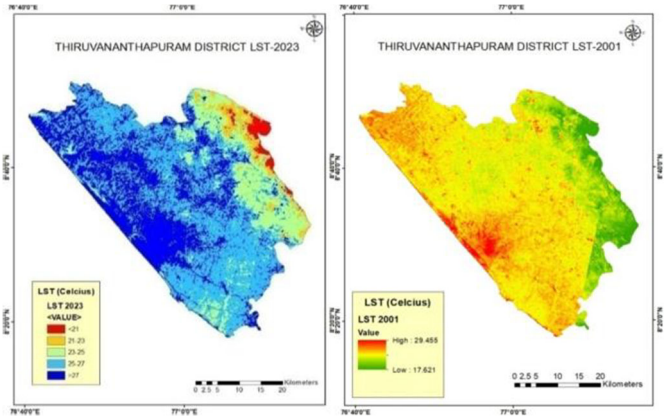

Fig. 3 Classified LST for (a) 2001 and (b) 2023

Validation is done for the LST retrieved from the satellite image. The obtained Land Surface Temperature is compared with the Air Temperature obtained from the Central Pollution Control Board web site (cpcb.nic.in). The difference is ≤ 0.5°C only.

Urban Thermal Field Variance Index (UTFVI)

The study area is classified into zones such as Excellent, Good, Normal, Bad, Worse and Worst according to thermal comfort. The variability experienced in the UTFVI index during the study period is shown in **Fig. 4**. The visual illustration of Excellent to Worse conditions is represented by Green to Indigo color scheme. There is a change in areas under the respective UTFVI zones over the following years. **Table 1** gives the area under the respective UTFVI zones. It can be inferred that during the year 2001, the area under excellent zones was 984.831 km². It decreased to 909.961km² during 2015 and further decreased to 888.191km² during 2023. There is a decrease of 9.81% of area over the 22 years. A drop of areas under good zones was observed over the span of years with a decrease of 14.37% of area. Area under normal zone showed a rise of 209.97%. An increase in the area under bad zone to 318.624% and worse zone to 185.830% is observed. A sharp increase in area under the worst zone is observed over the two decades which lead to a rise of 555.938% of area. The decline in thermal comfort within a short period of two decades in this area is alarming and has to be attended with immediate mitigation measures.

Table 1. Area under zones based on thermal comfort

UTFVI	EEI	2001	2015	2023	% change in area
None	Excellent	984.83	962.53	888.19	-9.81
Weak	Good	954.87	909.96	817.58	-14.37
Middle	Normal	84.93	139.16	263.28	209.97
Strong	Bad	14.01	24.18	58.68	318.62
Stronger	Worse	3.92	5.07	11.21	185.83
Strongest	Worst	0.652	2.33	4.28	555.93

Classification based on UTFVI

To have a better understanding, the study area was divided into different taluks. The villages under six different taluks of the study area were then classified based on UTFVI such as None, Weak, Middle Strong, Stronger and Strongest based on UHI phenomenon.
The least UTFVI effect was shown by the panchayats in Nedumangadu taluk. Larger area of the no category was showcased by Peringamala panchayat which is located in the easternmost side. This is due to the portion of Western Ghats located in the easternmost portion of Thiruvananthapuram district.

The taluks, such as Neyyatinkara, Kattakada and Varkala (**Table 2**) exhibited considerably a greater UTFVI effect. High UTFVI effect is observed in Chirayankeezhu taluk mainly because of increase in urbanisation and business activities. Majority of the area which are badly affected by UTFVI are found in the Thiruvananthapuram taluk which is an urban body where large business and commercial activities take place. The majority of the Strong, Stronger and the strongest area lies in the Thiruvananthapuram Taluk. Chakkai ward of Thiruvananthapuram showed the strongest UTFVI throughout the study period due to large bare area and low vegetation. The areas with the lowest values of NDVI, high built-up areas and higher NDBaI exhibited the increasing UTFVI effect.

Urban Hotspots (UHS)

Urban Hotpots significantly rise in locations with higher LST values. UHS for the years 2001, 2015 and 2023 were mapped as discussed in 3.2. The variation of UHS in the study area during the period is shown in **Fig. 5**. During the year 2001 the regions having threshold value greater than or equal to 25.218°Cwere considered as hotspots. Similarly in 2015 and 2023, threshold values of 27.407°C and 29.965°C were obtained.

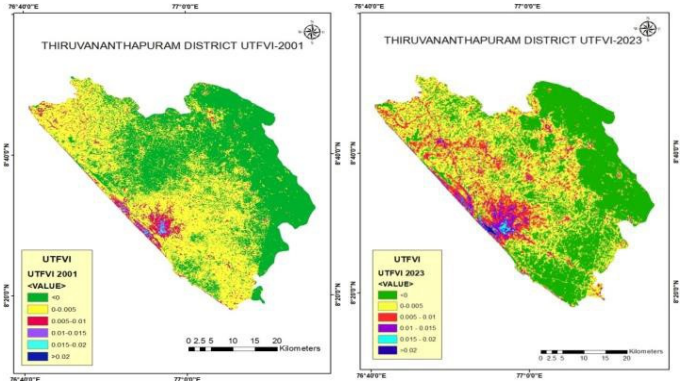

Fig. 4 UTFVI for (a) 2001 and (b) 2023

Table 2. Shifting of zones under UTFVI

Nedumangadu									
	Aryanad	Kallara	Nellanad	Panavoor	Peringamal	Pullanpara	Vamana puram	Vembayam	Vithura
2001	None	None	None	None	None	None	None	None	None
2015	None	Weak	Weak	Weak	None	None	Weak	None	None
2023	None	Weak	Middle	Weak	None	Weak	Weak	Weak	None
Neyyatinkara									
	Vellarada	Kunnathukal	Ottashekharamangalam	Vilappil	Kollayil	Perumkadavila			
2001	None	None	None	Weak	Weak	Weak			
2015	None	None	Weak	None	Weak	Weak			
2023	Weak	Weak	Weak	Weak	Weak	Weak			
Kattakada									
	Kallikade	Amboori	Kuttichal	Aaryancode	Poovachal				
2001	None	None	None	Weak	Weak				
2015	Weak	Middle	None	Weak	Weak				
2023	None	Weak	None	Weak	Middle				
Chirayankeezhu									
	Nagaroor	Vakkom	Karavaram	Anchuthengu	Attingal	Mudakkal			
2001	Weak	Weak	Weak	Middle	Middle	Middle			
2015	Weak	Middle	Weak	Middle	Middle	Middle			
2023	Middle	Middle	Middle	Strong	Strong	Middle			
Varkala									
	Madavoor	Pallikkal	Elakamon	Naavayikkulam	Edava				
2001	Weak	Weak	Weak	Weak	Weak				
2015	Weak	Weak	Weak	Weak	Weak				
2023	Weak	Weak	Weak	Middle	Middle				
Thiruvananthapuram									
	Thampanoor	Medical College	Paalkulangara	Palayam	Thycaud	Sreekandeshwaram			
2001	Strong	Middle	Middle	Strong	Middle	Strong			
2015	Strong	Middle	Middle	Strong	Middle	Strong			
2023	Stronger	Strong	Strong	Stronger	Strong	Stronger			
Coastal regions of Thiruvananthapuram									
	Vettukad	Valiyathura	Beemapally	Shankhumukham	Pallithura				
2001	Middle	Strong	Middle	Middle	Middle				
2015	Middle	Stronger	Strong	Middle	Strong				
2023	Strong	Stronger	Strong	Strong	Strong				

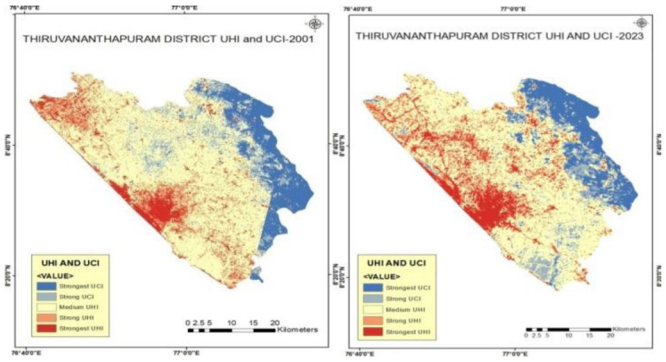

Fig. 5 UHI and UCI for (a) 2001 and (b) 2023

The results show that during 2001, the urban hotspots occupy an area of 34.178 km² i.e., 1.67% of the total area. There is an increase in the area to 45.758 sq. km in 2015. The areas identified as UHS were 2.24% of the total area. An increase of 11.58 km² UHS area is observed from 2001-2015. There is a decrease of area to 37.261km² observed during the period from 2015-2023. A decrease of 8.497km² of area observed during the period. A decrease of 1.82% of total area is observed. The hotspots identified as of 2023 are shown in **Fig. 6**. Higher concentration of UHS can be noticed in the Central Business district i.e., mainly the Thiruvananthapuram taluk. UHS can be seen in areas having lower vegetation and dense built-up area or in bare areas.

Mapping of LST of UHI and Non-UHI zones

The mapping of LST for different years in the two zones viz., UHI and Non-UHI zones are done (**Fig. 7**) as discussed in 3.2. The threshold value for UHI was found to be 22.04, 24.945 and 27.087 °C for 2001, 2015, and 2023 respectively. During the year 2001, the UHI zone covered an area of 448.125 sq. km whereas the Non-UHI zones covered an area of 1595.205km². The UHI zones constituted 21.9% of total area and Non –UHI zones covered 78.1% of the total area. During the year 2015 there was an increase in percentage of UHI zones. It increased to 26.81% and the non-UHI zones decreased from 78.1% to 73.19%. During the latest period of study, 30.61% of the total area is occupied by UHI zones and 69.39% is occupied by Non-UHI zones. The area covering the UHI and Non-UHI zones are listed in **Table 3.** The study area is classified into regions based on Urban Heat Islands (UHI) and Urban Cool Islands (UCI) as mentioned in section 3.2. The areas are classified as the regions having Strongest UCI, Strong UCI, Medium UHI, Strong UHI and Strongest UHI.

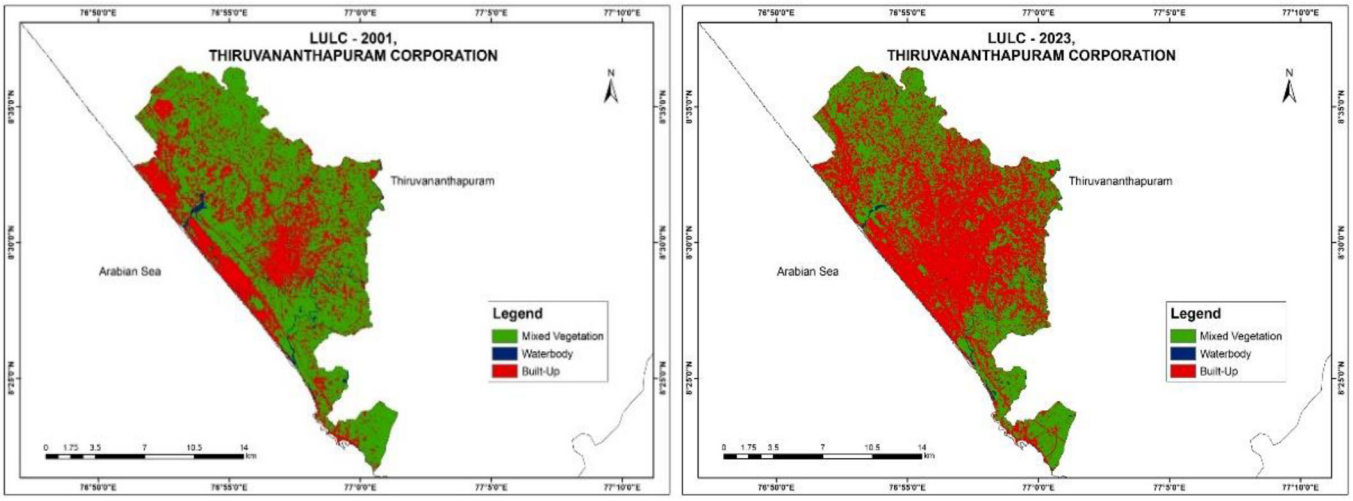

Fig. 6 LULC for (a) 2001 and (b) 2023

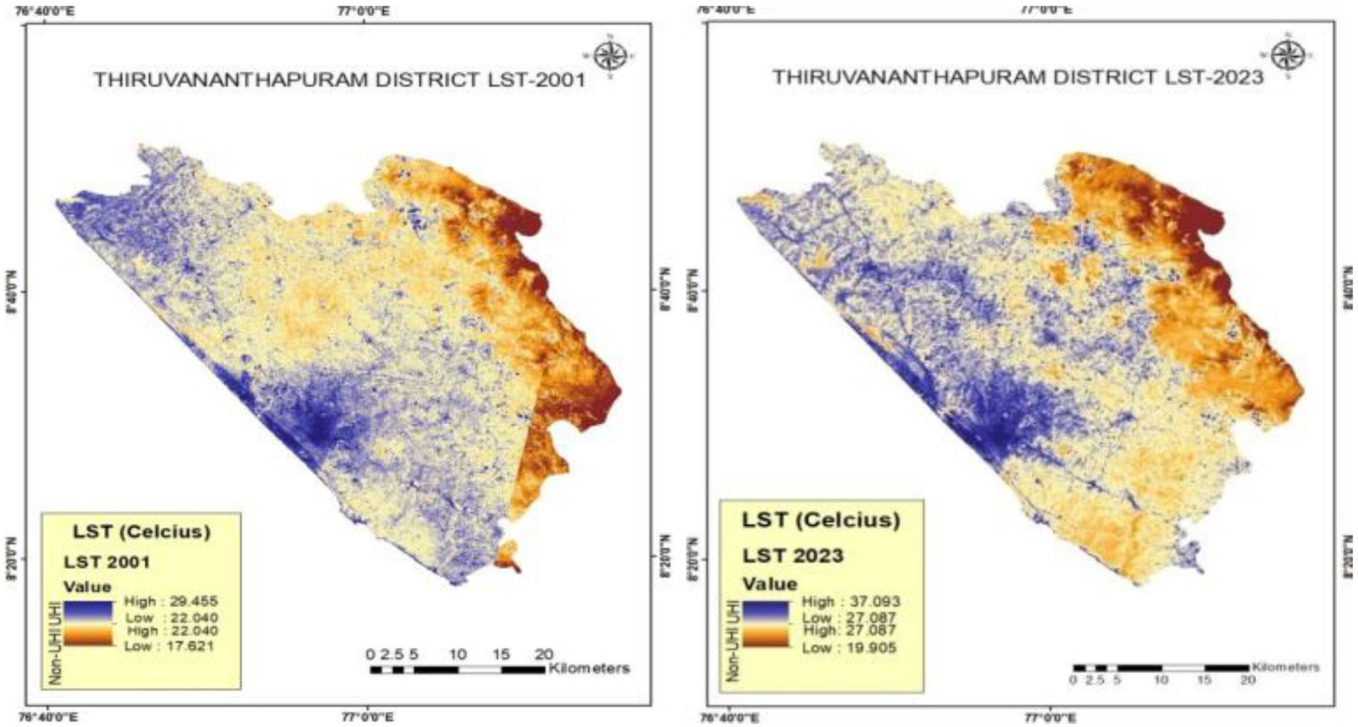

Fig. 7 UHI and Non-UHI for (a) 2001 and (b) 2023

Table 3. Area under UHI and Non-UHI zones

Zone	Area (km²)			Percentage of area (%)		
	2001	2015	2023	2001	2015	2023
UHI	448.125	547.966	625.443	21.9	26.81	30.61
Non-UHI	1595.20	1495.34	1417.88	78.1	73.19	69.39

Table 4 shows the area under UHI and UCI effect. There is an increase in area under strongest and strongest UHI zone from 2001 to 2023 by a value of 31.12% and 27.07% respectively. A decrease in medium UHI zone is observed by value of 16.21%. Negligible decrease in Strong UCI and a decrease in Strongest UCI zones are observed.

The UHI and UCI zones are classified in different taluks. The strongest UCI effect was observed in the Peringamala village of Nedumandagu. Majority of the regions exhibited a stronger UCI and a medium UCI/UHI. Most of the regions under Kattakada taluk exhibited a strong UCI to medium UCI/UHI. Neyyatinkara taluk exhibited a medium UCI/UHI. Medium to strong UHI was observed in Varkala. In Chirayankeezhu Taluk, the strongest UHI was observed in Anchuthengu. Thiruvananthapuram Taluk exhibited regions having medium to strongest UHI. The strongest UHI regions include the central business districts and the coastal regions.

LULC Change Analysis

The LULC maps for Thiruvananthapuram city was done for the years 2001 and 2023. From the LULC analysis it is was observed that over the period from 2001-2023, about 47.27 sq. km area has increased for built-up, i.e. 66 % increase in the area for built-up. The area for mixed vegetation has reduced to approximately 43.84 sq. km, i.e. 31% decrease in the area for mixed vegetation. Additionally, the area for water body has decreased to about 3.53 km², i.e., 68 % decrease in the area for water bodies.

Urbanization Proportion Index (UPI)

The UPI was calculated for Thiruvananthapuram city area for a period of 22 years from 2001-2023 and obtained a value of 21.98%. That is, the urban growth is quite active. That is the study area had a significant increase of urban growth over these years.

Land Use Indices

The Land use Indices are determined from the optical bands of the satellite images. Variation of indices such as NDVI, NDBI, NDBaI, MNDWI and NDMI were studied. The NDVI maps prepared for two decades, as discussed in 3.5.1 are shown in **Fig. 8**. The NDVI and LST showed a decreasing trend of 0.78 to 0.59 from 2001–2015 and a slight increase from 0.59 to 0.599 during 2015–2023. Negative values indicate the presence of water bodies. Lower NDVI value is observed on the Central Business region, mainly in the corporation area. Higher values are obtained on the outskirts of the city covering dense vegetation. The NDBI maps prepared as discussed on 3.5.2 are shown on **Fig. 9**.

The NDBI showed a high value of 0.88 during 2001. It decreased to 0.415 in 2015 and increased to 0.43 during 2023. NDBI is concentrated in the central part of the region. Increasing urbanization leads to the spread of built-up areas which decreases areas under vegetation and hence reduced moisture content. The NDBaI maps prepared as discussed in 3.5.3 is shown on **Fig. 10**.

The bare lands are areas having no vegetation. The NDBaI showed a low value of 0.268 during 2001. It increased to 0.349 in 2015 and decreased to 0.21 during 2023. An irregular variation is observed in NDBaI. High values of NDBaI are observed in the Chakkai ward of the Thiruvananthapuram Corporation. This is due to the presence of Thiruvananthapuram International Airport, where large area of bare land is present. The MNDWI maps prepared as discussed on 3.5.4 is shown on Fig.14.

The MNDWI showed a high value of 0.685 during 2001.It decreased to 0.347 in 2015 and slightly increased to 0.362 during 2023. The higher values indicate the presence of water bodies. The NDMI maps prepared as discussed in 3.5.5 are shown on **Fig. 11**.

NDMI increased from 0.387 in 2001 and increased to 0.426 in 2015. It showed a decreasing value of 0.406 in 2023. The barren land i.e., the Airport showed the lowest content of moisture as there is no vegetation present. High values are exhibited in regions having dense vegetation. A correlation analysis between parameters such as LST, Land Use Indices and Albedo was performed and resulted in ‘moderate’ to ‘good’ relation between variables.

Values greater than 0.6 were considered as ‘strong’, 0.4 to 0.6 as ‘moderate’ and less than 0.4 as ‘poor’. NDVI, MNDWI and NDMI are decreasing with LST. Indices such as NDBI, NDBaI and Albedo has clearly ‘moderate’ to ‘strong’ positive correlation (0.40-0.65)

Table 4. Area under UHI and UCI effect

UHI effect	Area (km²)			% change in years
	2001	2015	2023	
Strongest UHI	165,347	204,94	239,73	31,12
Strong UHI	281,16	342,828	385,522	27,07
Medium UHI	1117,983	1045,501	962,033	-16,21
Strong UCI	197,83	222,329	199,332	-0,76
Strongest UCI	280,951	227,647	256,64	-9,47

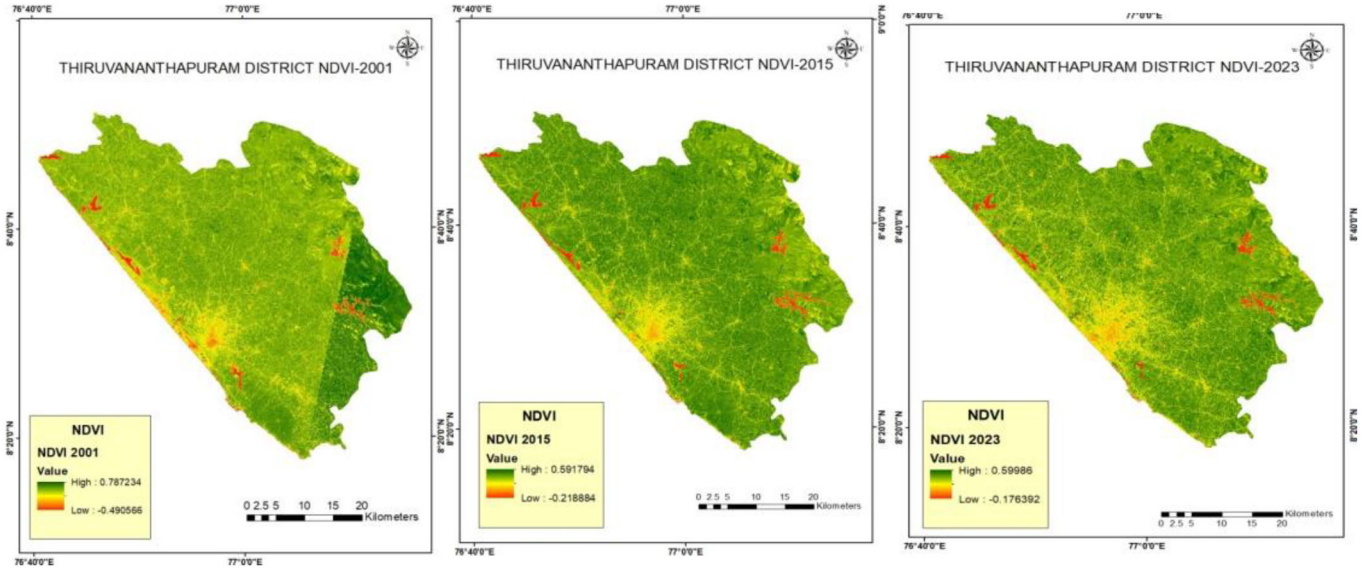

Fig. 8 NDVI for (a) 2001, (b) 2015, and (c) 2023

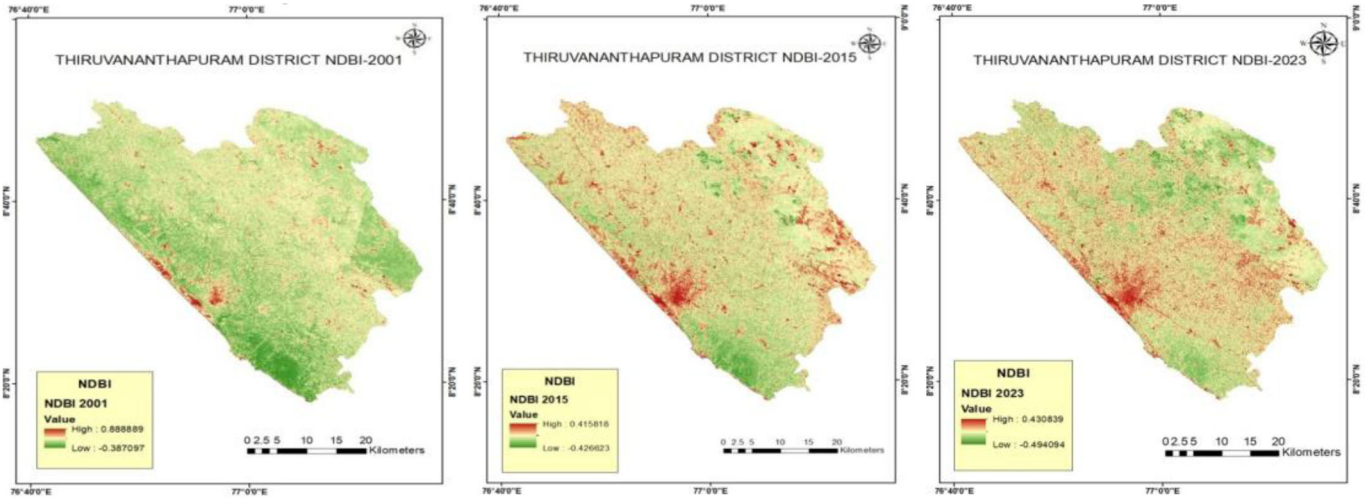

Fig. 9 NDBI for (a) 2001, (b) 2015, and (c) 2023

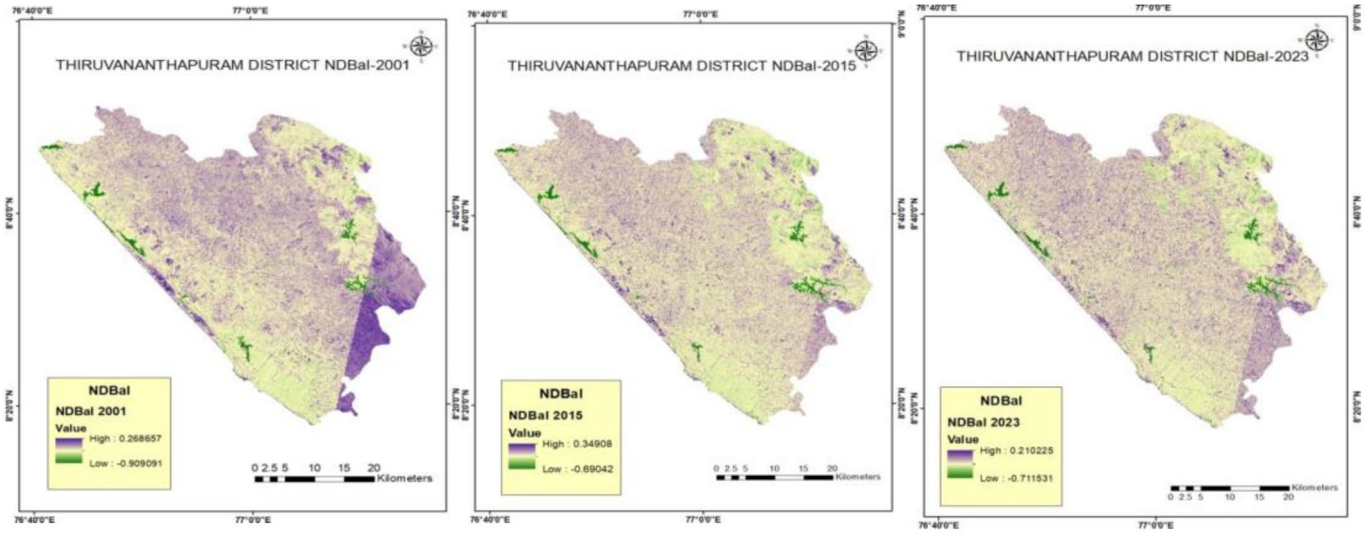

Fig. 10 NDBaI for (a) 2001, (b) 2015, and (c) 2023

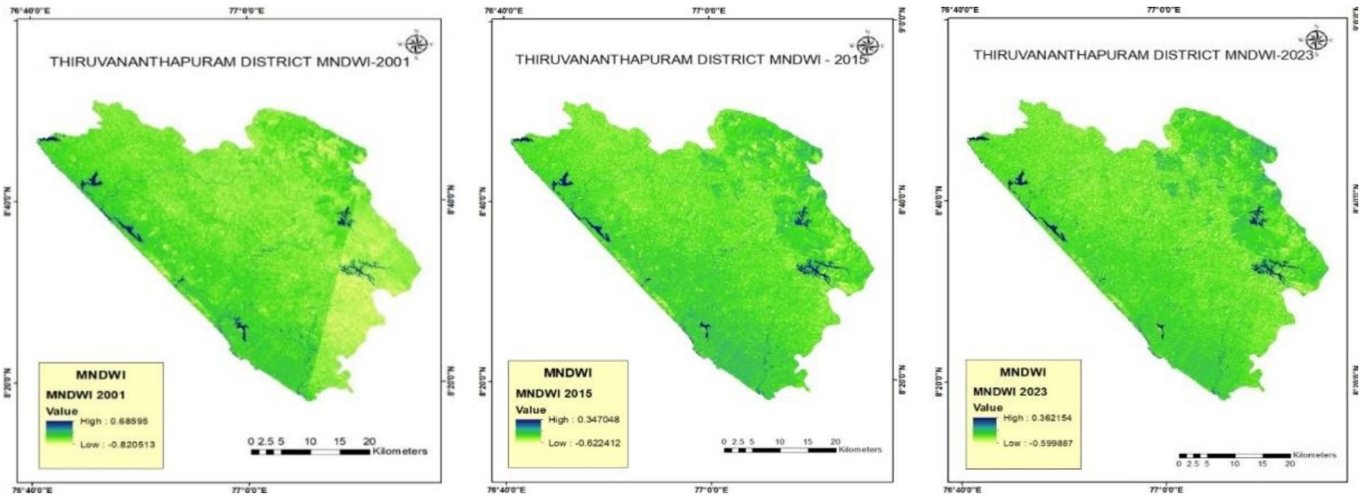

Fig. 11 MNDWI for (a) 2001, (b) 2015, and (c) 2023

with LST. NDVI is found to be inversely related to NDBI in a 'strong' way. NDBI and NDMI showed a correlation of unity. NDBaI has strong negative correlations with MNDWI and a moderate negative correlation with NDMI.

Regression Analysis with LST

A Multivariate Linear Regression model is developed with Land use indices and albedo with LST. The equation obtained is:

LST = 24.423 - 6.741 MNDWI - 14.415 NDVI + 39.657 ALBEDO

The independent variables are statistically significant for the prediction of the dependent variable. The value of the unstandardized coefficient illustrates the correlation between value of MNDWI and NDVI denotes that it varies negatively with LST whereas the positive value of Albedo implies that it varies positively with LST.MNDWI, Albedo and NDVI are significant predictors of LST. Albedo had a greater impact on the LST as indicated by the standardised coefficients based on the magnitude of the t-statistics. 80% of the sample data were used to develop the model and 20% were used for validation. An RMSE value of 1.26 was obtained.

CONCLUSIONS

Landsat images are highly useful for assessing the LST, LULC and Land Use Indices such as NDVI, NDBI, NDBaI, MNDWI and NDMI as well as Albedo. The urban thermal environment exhibited a remarkable increase in the worst areas under the UTFVI classification thus reducing the ecological quality.There is a rapid increase area under the strongest UTFVI which is mainly concentrated in the Central Business part of the district. High LST, therefore greater UHI effect is observed in the Central Business District. LST was found to be high in the built up and barren regions and was found to be low in the agricultural, vegetated areas and lowest in the water bodies. The Urban hotspots are concentrated in the built up and bare area of the Thiruvananathapuram taluk which also exhibited profound effect of UHI. Chakkai ward shows the strongest UHI effect in Thiruvananthapuram district due to large area of barren land and low vegetation which was due to the presence of Trivandrum International Airport. The regions under urban cool Islands are identified as Peringamala panchayat of Nedumangadu taluk which is the easternmost region of the study area. The proximity of Western Ghats may be the reason for the cooling effect in the region. A multivariate linear regression model is very useful for predicting the land surface temperature. NDVI, MNDWI and Albedo are the parameters that were highly influenced by LST in the study area. LULC and urbanization proportion index showed a significant urban growth over these years which is also a reason for the increase which is also a reason for the increase of LST in the study area.

REFERENCES

Kusumawardani and Hidayati., 2023. Analysis of urban heat island and urban ecological quality based on remote sensing imagery transformation in semarang city. IOP Conf. Series: Earth and Environmental Science.

Rendana M., Mohd W. R. I., Abdul S. R., Ghassan H, A., Almohamad H., Abdullah A. D. et.al, 2023. Relationships between land use types and urban heat island intensity in Hulu Langat district, Selangor, Malaysia. Ecological Process:12, 33.

Sharma S., Hussain S., and Singh A. N., 2023. Impact of Land Use and Land Cover On Urban Ecosystem Service Value In Chandigarh, India: A GIS-Based Analysis. Journal of Urban Ecology, 9(1).

Tesfamariam S., Govindu V., and Uncha A., 2023. Spatio- temporal analysis of urban heat island (UHI) and its effect on urban ecology: The case of Mekelle city, Northern Ethiopia,. Heliyon 9(2).

Guha S., Govil H., Kumar A. T., Gill N., and Dey A., 2022. Land surface temperature and spectral indices: A seasonal study of Raipur City. Geodesy and Geodynamics, 13(1), 72-82.

Basheer S., Wang X., Farooque A. A., Nawaz R. A., Liu K., Adekanmbi T., and Liu S., 2022. Comparison of Land Use Land Cover Classifiers Using Different Satellite Imagery and Machine Learning Techniques. Remote Sensing, 14(19).

Kalogeropoulos G., Dimoudi A., Toumboulidis P., and Zoras S., 2022. Urban Heat Island and Thermal Comfort Assessment in a Medium-Sized Mediterranean City. Atmosphere, 13(7):1102.

Li X., Stringer L. C., and Dallimer M., 2022. The Impacts of Urbanisation and Climate Change on the Urban Thermal Environment in Africa. Climate, 10(11):164.

Badasa M., Niguse I. D., Reta Z. R., and Obsi D G., 2022. Impact of urban land use and land cover change on urban heat island and urban thermal comfort level: a case study of Addis Ababa City, Ethiopia. Environmental Monitoring and Assessment:194:736.

Pandey A., Mondal A., Guha S., Kumar P. U., and Singh D., 2022. Land use status and its impact on land surface temperature in Imphal city, India. Geology, Ecology, and Landscapes. https://doi.org/10.1080/24749508.2022.2131962

Rashid N., Mostahidul J. A. M. A., Chowdhury A., and Labib, S. U. I., 2022. Impact of land use change and urbanization on urban heat island effect in Narayanganj city, Bangladesh: A remote sensing-based estimation. Environmental Challenges:8.

Sidiqui P., Roos P. B., Herron M., Jones D. S., Duncan E., Jalali, A. et.al,2022. Urban Heat Island vulnerability mapping using advanced GIS data and tools. J. Earth Syst. Sci.131:266.

Vahmani P., Luo X., Jones A., and Hong T., 2022. Anthropogenic heating of the urban environment: An investigation of feedback dynamics between urban micro- climate and decomposed anthropogenic heating from buildings. Building and Environment:213.

Abir F. A., Ahmmed S., Hossain S. S., and Uddin A. F., 2021. Thermal and ecological assessment based on land surface temperature and quantifying multivariate controlling factors in Bogura, Bangladesh. Heliyon:7(9).

Abulibdeh A., 2021. Analysis of urban heat island characteristics and mitigation strategies for eight arid and semi-arid gulf region cities. Environmental Earth Sciences. 80. 10.1007/s12665-021-09540-7.

Almeida C. R., Teodoro A. C, and Gonçalves. A 2021. Study of the Urban Heat Island (UHI) Using Remote Sensing Data/Techniques: A Systematic Review. Environments, 8(10):105.

Ayanlade A., Aigbiremolen M., and Oladosu O. R., 2021. Variations in urban land surface temperature intensity over four cities in diferent ecological zones. Scientific Reports: 11:20537.

Faisal A. A., Kafy A. A., Rakib A. A., Shaleha,K A., Amir, D. J., and Sikdar S., 2021. Assessing and predicting land use/land cover, land surface temperature and urban thermal field variance index using Landsat imagery for Dhaka Metropolitan area. Environmental Challenges:4.

Khan M. S., Ullah S., and Chen L., 2021. Comparison on Land-Use/Land-Cover Indices in Explaining Land Surface Temperature Variations in the City of Beijing, China. Land 10, 1018. http://dx.doi.org/10.3390/land10101018

Kumar A., Agarwal V., Pal L., Kumar S. C., and Mishra V., 2021. Effect of Land Surface Temperature on Urban Heat Island in Varanasi City, India. Multidisciplinary Scientific Journal, 4(3),420–429. http://dx.doi.org/10.3390/j4030032

Maharjan M., Aryal A., Man B. S., Talchabhadel R., Raj B. T., and Kumar S., 2021. Evaluation of Urban Heat Island (UHI) Using Satellite Images in Densely Populated Cities of South Asia. Earth 2(1), 86–110. http://dx.doi.org/10.3390/earth2010006

Naim N. H., and Kafy A., 2021. Assessment of urban thermal field variance index and defining the relationship between land cover and surface temperature in Chattogram city: A remote sensing and statistical approach. Environmental Challenges:4.

Shahfahad., Talukdar S., Rihan M., and Hang H. T., 2021. Modelling urban heat island (UHI) and thermal field variation and their relationship with land use indices over Delhi and Mumbai metro cities. Environment, Development and Sustainability:24(4).

Tepanosyan G., Muradyan V., Hovsepyan A., Pinigin G., Medvedev A., and Asmaryan S., 2021. Studying spatial- temporal changes and relationship of land cover and surface Urban Heat Island derived through remote sensing in Yerevan, Armenia. Building and Environment:187.

Palanisamy A., Padmalal D and Maya K. K., 2020. Impact of urbanization and land surface temperature changes in a coastal town in Kerala,India. Environmental Earth Science:79(17).

Elmarakby E and Elkadi H., 2020. Spatial Morphology and Urban Heat Island: Comparative Case Studies. https://doi.org/10.1007/978-3-030-52584-2_31

Mmustafa E., Liu G., Cao Y., and Kaloop M., 2020. Study for Predicting Land Surface Temperature (LST) Using Landsat Data: A Comparison of Four Algorithms. Advances in Civil Engineering.

Omali T., 2020. Ecological Evaluation of Urban Heat Island Impacts in Abuja Municipal Area of FCT Abuja, Nigeria. World Academics Journal of Engineering Sciences, 7(1), 66-72.

Peng X., Wu W., Zheng Y., Sun J., Hu T., and Wang P., 2020. Correlation analysis of land surface temperature and topographic elements in Hangzhou, China. Scientific Reports:10(1).

Raj S., Kumar S. P., Chakraborty A., and Kuttippurath J., 2020. Anthropogenic forcing exacerbating the urban heat islands in India. Journal of Environmental Management, 257.

Sharma R., Pradhan L., Kumari M., and Bhattacharya P., 2020. Assessing urban heat islands and thermal comfort in Noida City using geospatial technology. Urban Climate:35.

Sulthana S., and Satyanarayana A. N. V., 2018. Urban heat island intensity during winter over metropolitan cities of India using remote-sensing techniques: impact of urbanization. International Journal of Remote Sensing, 39(20).

Kikon N., Singh P., Kumar S. S., and Vyas A., 2017. Assessment of urban heat islands (UHI) of Noida City, India using multi-temporal satellite. Sustainable Cities and Society:22, 19-28.

Satheendran S., Chandran S., and Varghese A. 2018. Space Based Spatio-Temporal Assessment of Land Surface Temperature in Karunagappally Municipality, a Fast Growing City in the Western Coast of India. The International Archives of the Photogrammetry, Remote Sensing and Spatial Information Sciences:42(5).

Suja R., Letha J., and Varghese J., 2013. Evaluation of Urban Growth and Expansion using Remote Sensing and GIS. International Journal of Engineering Research & Technology (IJERT), 2(10).

Rahman A., Kumar S., Fazal S., and Siddiqui M. A., 2012. Assessment of Land Use/Land Cover Change in the North- West District of Delhi Using Remote Sensing and GIS Techniques. Journal of the Indian Society of Remote Sensing, 40(4), 689-697.